Orthorhombic fulleride $(CH_3NH_2)K_3C_{60}$ close to Mott-Hubbard instability: *Ab initio* study

Anton Potočnik,[1,*] Nicola Manini,[2,3,4,†] Matej Komelj,[1] Erio Tosatti,[3,4,5,‡] and Denis Arčon[1,6]

[1]*Condensed Matter Physics Department, Jožef Stefan Institute, Jamova cesta 39, SI-1000 Ljubljana, Slovenia*

[2]*Dipartimento di Fisica, Università degli Studi di Milano, via Celoria 16, 20133 Milano, Italy*

[3]*Scuola Internazionale Superiore di Studi Avanzati (SISSA), Via Bonomea 265, 34136 Trieste, Italy*

[4]*CNR-IOM Democritos, Via Bonomea 265, 34136 Trieste, Italy*

[5]*International Centre for Theoretical Physics (ICTP), Strada Costiera 11, 34151 Trieste, Italy*

[6]*Faculty of mathematics and physics, University of Ljubljana, Jadranska 19, SI-1000 Ljubljana, Slovenia*

(Received 11 June 2012; published 8 August 2012)

We study the electronic structure and magnetic interactions in methylamine-intercalated orthorhombic alkali-doped fullerene $(CH_3NH_2)K_3C_{60}$ within the density functional theory. As in the simpler ammonia intercalated compound $(NH_3)K_3C_{60}$, the orthorhombic crystal-field anisotropy Δ lifts the t_{1u} triple degeneracy at the Γ point and drives the system deep into the Mott-insulating phase. However, the computed Δ and conduction electron bandwidth W cannot alone account for the abnormally low experimental Néel temperature, $T_N = 11$ K, of the methylamine compound, compared to the much higher value $T_N = 40$ K of the ammonia one. Significant interactions between CH_3NH_2 and C_{60}^{3-} are responsible for the stabilization of particular fullerene-cage distortions and the ensuing low-spin $S = 1/2$ state. These interactions also seem to affect the magnetic properties, as interfullerene exchange interactions depend on the relative orientation of deformations of neighboring C_{60}^{3-} molecules. For the ferro-orientational order of CH_3NH_2-K^+ groups we find an apparent reduced dimensionality in magnetic exchange interactions, which may explain the suppressed Néel temperature. The disorder in exchange interactions caused by orientational disorder of CH_3NH_2-K^+ groups could further contribute to this suppression.

DOI: 10.1103/PhysRevB.86.085109 PACS number(s): 71.20.Tx, 74.70.Wz, 71.30.+h

I. INTRODUCTION

The alkali-doped cubic fullerides ($A_{3-x}A'_xC_{60}$, A, A' = Na, K, Rb, Cs) are prominent members of a rapidly growing family of π-electron organic superconductors[1] with superconducting transition temperature, T_c, as high as 38 K.[2,3] In the early days of fullerene research the observed monotonic increase of T_c as a function of unit-cell volume was attributed to the increased density of states at the Fermi level, within a standard Bardeen-Cooper-Schrieffer (BCS) theory.[4] Due to the threefold degeneracy of the t_{1u}-derived bands at the Γ point, preserved in cubic structures, and to the well-established vibron coupling, the Jahn-Teller (JT) effect is believed to participate actively in the superconducting pairing mechanism.[5] However, since the conduction electron's bandwidth (W) and the on-site Coulomb repulsion energy (U) are comparable, it was also argued that fullerides must be very close to a Mott-Hubbard transition.[6] Phase transitions from a superconducting to a Mott insulating state were indeed demonstrated long ago upon intercalation-induced lattice expansion in compounds such as $(NH_3)K_3C_{60}$[7] where, similarly to $Li_3(NH_3)_6C_{60}$,[8] expansion increases the repulsion/bandwidth ratio U/W, raising the importance of correlations. These notions recently received strong support with the discovery of Cs_3C_{60}, a cubic fulleride with the largest unit cell and low-spin ($S = 1/2$) antiferromagnetic Mott-insulating ground state at ambient pressure conditions[2,9–13] and where high-temperature superconductivity is revived under hydrostatic pressure with no structural symmetry change. Strikingly, under pressure here T_c displays a dome-like unit-cell volume dependence typical of unconventional superconductors,[14] frankly inexplicable within BCS, Migdal-Eliashberg, and related weakly interacting models. Conversely, precisely such a nonmonotonic behavior of T_c had been predicted by dynamical mean field theory (DMFT) for the unconventional superconducting phase bordering a Mott-insulating state at large unit-cell volumes in a simple three-band Hubbard model incorporating, besides a JT electron-vibron coupling, strong on-site electron correlations, caused both by the Coulomb repulsion and by Hund's rule exchange, J_H.[15] That success not only highlights the unconventional interplay of strong correlations and phonons in these systems, but it also brings expanded alkali-doped fullerenes at the forefront of the strongly correlated electron systems and superconductors, where good understanding of one model system may help shed more light on the entire highly controversial field.

In search for higher transition temperatures, earlier approaches toward expanded unit cells had been by means of co-intercalation of inert ammonia (NH_3), e.g., $NH_3K_{3-x}Rb_xC_{60}$ ($x = 0,1,2,3$)[16,17] and in $Li_3(NH_3)_6C_{60}$,[8] or of methylamine (MA) molecules, in $(CH_3NH_2)K_3C_{60}$ (MAK_3C_{60}).[18] These molecules operate as spacers between C_{60} molecules and are believed to have negligible direct influence on the electronically active t_{1u} molecular orbitals of C_{60}^{3-} anions. However, their presence breaks the original cubic symmetry, resulting in orthorhombic crystal structures and effectively lifting the threefold degeneracy of the t_{1u}-derived bands at the Γ point. This splitting reduces the critical value for U/W_c,[19] immediately pushing noncubic fullerides over the metal-insulator transition (MIT) boundary.[7,20] We stress that these anisotropic compounds would still be metals, presumably also BCS superconductors, if strong on-site electron correlations were not present.[20] They are thus important model systems for investigations of correlation effects in metals where the splitting of the originally degenerate narrow bands can be tuned through the anisotropy field.

At low temperatures $NH_3K_{3-x}Rb_xC_{60}$ compounds order to an antiferromagnetic insulating state with Néel temperature T_N, ranging from 40 K to the maximum of 80 K for $x = 0$ and $x = 2$, respectively.[16,21] MAK_3C_{60}, on the other hand, orders to an antiferromagnetic state at remarkably lower $T_N = 11$ K.[22] Assuming that the electronic properties depend mainly on the unit-cell volume, one would anticipate T_N to be ∼80 K, i.e., similar to that of $NH_3KRb_2C_{60}$. Such profoundly different magnetic response to different co-intercalands is unexpected and implies that in addition to direct interfullerene electronic overlap also other degrees of freedom play a role in noncubic fullerides. We first note that the c/a lattice parameter ratio is smaller in MAK_3C_{60} than in $NH_3K_{3-x}Rb_xC_{60}$, where it is closer to unity.[16,18] Therefore, the difference between the two orthorhombic compounds may arise from the different orthorhombic anisotropy field Δ. In other words, properties of MAK_3C_{60} and $NH_3K_{3-x}Rb_xC_{60}$ compounds are fine-tuned by the closeness to the Mott-Hubbard boundary on the (U,Δ) Manini-Santoro-Dal Corso-Tosatti (MSDT) phase diagram for fullerides.[20] While it is well established that $NH_3K_3C_{60}$ lies very close to this boundary, the precise position of MAK_3C_{60} is yet to be determined.

In cubic fullerides the high crystal symmetry prevents ordering of the t_{1u} molecular orbitals; i.e., it is believed that cubic A_3C_{60} are in an orbitally liquid state,[4] at least above the antiferromagnetic Néel temperature. In the noncubic fullerides, however, one expects that a crystal field will select a particular C_{60}^{3-} cage distortion and thus would also affect the interfulleride hopping integrals. Since the MA molecule is rather large compared to available octahedral space in the fulleride structure, a strong interaction, presumably even the formation of a weak hydrogen bond, between the MA-K^+ group and the nearest C_{60} was proposed.[18] MAK_3C_{60} thus offers a unique opportunity to investigate the role of symmetry breaking on the JT effect in strongly correlated electron systems. Stimulated by these open issues we decided to carry out a systematic *ab initio* study of MAK_3C_{60} by the density functional theory (DFT) in the local density approximation (LDA), where even if strong correlations are treated only at the mean-field level, the detailed chemical bonding and crystal-field strengths can be assessed. We show that the crystal-field anisotropy of MAK_3C_{60} is larger compared to $NH_3K_3C_{60}$, thus placing it deeper in the insulating region of the phase diagram. The whole electron-hopping structure is found to be significantly affected by the MA insertion. We find evidence for the presence of strong C_{60}^{3-} steric effect that may lead to a reduced dimensionality in magnetic exchange interactions and explain suppressed T_N.

II. METHODS

We execute DFT calculations using the Quantum Espresso software package (pwscf program).[23] Ultrasoft pseudopotentials appropriate for the Perdew-Zunger exchange correlation (LDA) are used. The pseudo-Bloch functions are expanded over plane waves with an energy cutoff of 50 Ry on a 5^3 Monkhorst-Pack k-space mesh, such that the total energy is within 250 meV of its converged value, while the conduction bands are within 0.1 meV of their converged value. The Fermi surface is smeared with a "temperature" parameter of 2 meV using the Gaussian smearing method. The density of states (DOS) is evaluated with the tetrahedron method, sampling k space with a uniform 8^3 mesh. For the relaxation of the atomic positions, we adopt a damp (quick-min Verlet) procedure on a 2^3 k-space mesh with a plane-wave energy cutoff of 30 Ry and the same smearing of the Fermi surface. The maximally localized Wannier orbitals are obtained using the Wannier90 package.[24] The three Wannier orbitals are computed in the t_{1u} energy window, using 5^3 k points on a Monkhorst-Pack grid with Bloch phases as initial projections. All three Wannier orbitals are positioned on the central C_{60} molecule and have a similar spread of $\sqrt{\Omega} \sim 0.4$ nm. We tested the convergence of Wannier orbitals' hopping integrals as a function of the number of k points, and negligible changes of less than 0.01 meV are found for k-space mesh finer than 5^3. The projected DOS (PDOS) on the three Wannier orbitals were evaluated using the Gaussian smearing method with a "temperature" parameter of 8 meV. The use of two different methods for evaluation of DOS and PDOS gives rise to a slight mismatch between the two. The mismatch does not affect the conclusions of this work.

III. RESULTS AND DISCUSSION

A. Phase diagram

The MAK_3C_{60} compound grows in the face-centered orthorhombic (space group *Fmmm*) crystal structure with the room-temperature unit-cell parameters $a = 15.2027$ Å, $b = 15.1800$ Å, and $c = 13.5032$ Å ($V = 779.057$ Å^3).[18] The MA-K^+ groups situated only in the large octahedral sites were found to be dynamically disordered between eight equivalent orientations at high temperatures.[25] Below the structural phase transition at $T_s = 220$ K MA-K^+ groups become static and probably ordered in an (anti)ferro-orientational order similar to $NH_3K_3C_{60}$.[26] Since the details of the low-temperature structure are not known yet we base all our band-structure calculations on the experimental room-temperature structure. We select a single MA-K^+ orientation, thus effectively imposing a ferro-orientational order of the MA-K^+ groups.

The three metallic t_{1u} bands are well isolated from other molecular orbital-derived bands as is the case with every fullerene compound.[27] The band gap between "C_{60} HOMO" (h_u-derived bands) and "C_{60} LUMO" (t_{1u}-derived bands) is 0.96 eV, while the separation between "C_{60} LUMO" and "C_{60} LUMO + 1" (t_{1g}-derived bands) is 0.59 eV. For comparison we refer here to the corresponding gaps of 1.16 and 0.38 eV computed for cubic K_3C_{60},[28] and to the experimental values, roughly 1.8 and 1 eV, respectively.[29] The underestimation of the band gaps, standard for LDA calculations, is fortunately of little consequence in our case. The neat separation of the different band groups allows us to focus entirely on t_{1u}-derived bands close to the Fermi energy (Fig. 1). Not surprisingly, bare DFT-LDA nonmagnetic calculations yield for MAK_3C_{60} a metallic ground state with a half-filled t_{1u} band. However, several experiments proved that MAK_3C_{60} is an insulator,[22,25,30,31] clearly suggesting that the mean-field DFT metallic state is driven to a Mott-Hubbard insulating state by electron correlations. Since the phase diagram for

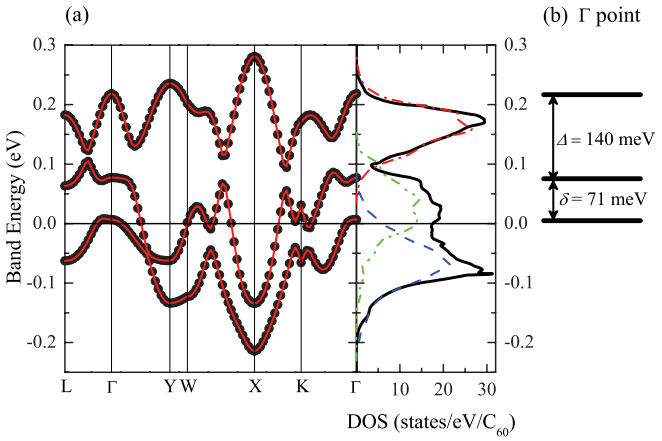

FIG. 1. (Color online) (a) Band structure and DOS for the room temperature MAK_3C_{60} crystal structure. Red solid line is the interpolated band structure using the maximally localized Wannier orbitals; see text for details. Black solid line is the total DOS; the red dot-dashed line, green dash-dot-dotted line, and blue dashed line represent the PDOS on the first, second, and the third Wannier orbital, respectively. (b) The splitting of t_{1u} bands at the Γ point, defining the orthorhombic crystal-field anisotropy.

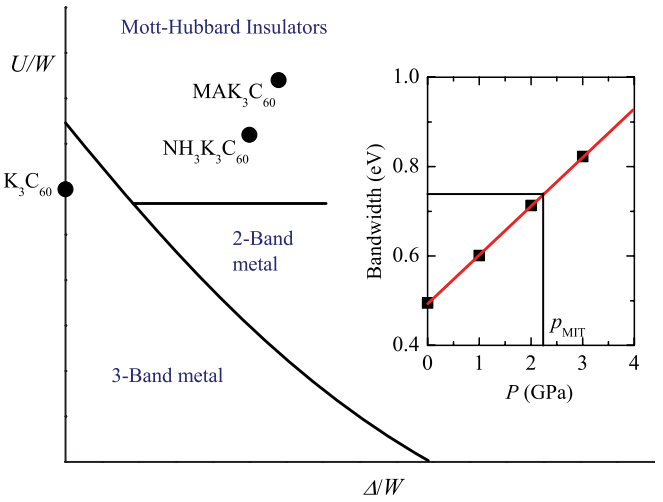

FIG. 2. (Color online) MSDT phase diagram for fullerides adapted from Ref. 20 including MAK_3C_{60} position. Inset: Pressure dependence of the bandwidth computed for the room-temperature MAK_3C_{60} structure. The horizontal line marks the critical bandwidth 0.74 eV where $(U/W)_c = 1.35$ and where metal-insulator transition is expected.

noncubic fullerides has already been calculated within DMFT with included electron correlations, it is sufficient at this stage to continue the characterization of MAK_3C_{60} in the noncorrelated limit and then treat electron correlations, e.g., within the established MSDT phase diagram.[20]

Orthorhombic crystal symmetry is reflected in the band structure [Fig. 1(a)] by (1) the removal of the threefold degeneracy at the Γ point [Fig. 1(b)] and (2) the inequivalence of Y and X points. At the Γ point we compute an energy splitting between the first and the second and between the second and the third t_{1u} energy levels of $\delta = 71$ meV and $\Delta = 140$ meV, respectively. For comparison, the corresponding energy splittings for $NH_3K_3C_{60}$ are $\delta \approx 30$ meV and $\Delta \approx 150$ eV.[20] In general, Δ reflects the main orthorhombic crystal-field anisotropy and δ tracks the smaller anisotropy in the ab plane. Surprisingly, band-structure anisotropies of the two systems are very much comparable despite some obvious crystallographic differences, like, for instance, the ratio c/a, which is 0.89 and 0.91 for MAK_3C_{60} and $NH_3K_3C_{60}$, respectively. In order to position MAK_3C_{60} on the MSDT phase diagram we need to evaluate W, which is deduced directly from the computed band structure. The resulting total t_{1u} DOS, roughly shaped in three peaks and shown in Fig. 1(a), resembles that of $NH_3K_3C_{60}$.[20] We note that the apparent disagreement between DOS width and the band-structure splitting at the X point is due to very a small number of states at extreme values, and it can thus be seen only in the zoomed view for small DOS values. We obtain a quite large DOS at the Fermi energy, $N(E_F) = 17$ states/eV/C_{60}, which is a result of expanded lattice structure and the resulting smaller bandwidth $W = 0.5$ eV. For comparison, we refer here to the $W \approx 0.6$ eV reported for $NH_3K_3C_{60}$ and K_3C_{60}, which are characterized by smaller unit cells.[20]

The above results bring forward two interesting aspects of the MA cointercalation. The first is the position of MAK_3C_{60} on the MSDT phase diagram. Manini *et al.*[20] used Δ/W as a measure of the anisotropy, which also defines the distance to the MIT boundary in noncubic fullerides. Based on $\Delta/W \approx 0.25$ $NH_3K_3C_{60}$ is quite close to both two- and three- band metallic phases. It is thus expected that under pressure $NH_3K_3C_{60}$ would almost instantly end up in one of these two metallic states. We find MAK_3C_{60} to be slightly more anisotropic, judging from $\Delta/W = 0.29$, thus deeper in the Mott-insulating phase and further away from the three-band metallic phase (Fig. 2).

Application of a hydrostatic pressure, a standard experimental method for increasing W and thus pushing systems across the metal-insulator boundary, has yet to be attempted in magnetic-resonance experiments to verify our calculations. However, based on the above observation, we predict that larger pressures will be needed in MAK_3C_{60} to access metallic and possibly superconducting states. To estimate the required metal-insulator transition pressure in MAK_3C_{60} we compute the bandwidth as a function of decreasing unit-cell volume, mimicking the effect of an external pressure. The pressure dependence of the unit-cell parameters was taken from the high-resolution x-ray data measured under hydrostatic conditions.[32] To prevent unphysical contact between C_{60} and MA groups we carried out a structural optimization for each volume. The bandwidth increases monotonically with decreasing unit-cell volume, or increasing pressure, with the slope of $dW/dP = 100$ meV/GPa (inset of Fig. 2). If the effect of pressure could be reduced only to a pressure dependence of W, we would predict a steep increase of T_N in the insulating phase as a function of pressure, estimating, for instance, $T_N(1\text{ GPa})/T_N(0) \sim (W/W_0)^2 = 1.44$. At higher pressures insulator-metal instability is expected to occur. If we take critical ratio $(U/W)_c = 1.35$ as appropriate for the orthorhombic structure[20] and a typical value for fullerenes $U = 1$ eV,[4] we predict that this transition should take place at around $p_{MIT} = 2.3$ GPa. Nonlinear effects on compressibility may push this critical pressure slightly higher.

Contrasted with the metal-insulator transition, magnetic ordering cannot be understood purely in terms of overall properties such as the bandwidth or crystal-field anisotropy. In particular, the abnormally small $T_N = 11$ K of MAK_3C_{60} as compared with $T_N = 40$ K for $NH_3K_3C_{60}$ can hardly be justified by the fairly small differences either in the bandwidth or in the orthorhombic anisotropy. Accordingly, the lattice expansion alone cannot explain the small T_N: The antiferromagnetic ordering must be controlled by other degrees of freedom such as the interaction between co-intercaland molecules and C_{60}^{3-} anions and the related stabilization of a particular JT deformation. We will test this hypothesis in the following sections.

B. The Jahn-Teller effect

Let us focus first on JT effect of C_{60}^{3-} anion, which has been predicted[33] but has been experimentally much more elusive in fullerene systems.[34] Orthorhombic crystal structures should provide a fertile ground for JT effect investigations. In order to isolate JT effect we consider an artificial enlarged face centered orthorhombic C_{60}^{3-} structure using the room-temperature MAK_3C_{60} lattice parameters multiplied by a factor of 1.5. To ensure charge neutrality, we add a uniform positive background in the DFT calculation. This positive background is not contributing to the orthorhombic crystal field, and therefore any removal of t_{1u} degeneracy at the Γ point should arise solely from the JT effect on top of the weak residual crystal field from the periodically replicated C_{60}^{3-} ions. The positions of C_{60} carbon atoms were relaxed in order to obtain molecular distortions. The C_{60}^{3-} ion deforms spontaneously into a structure with D_{2h} symmetry [Fig. 3(a)]. This is the expected symmetry for $t_{1u} \otimes H_g$ JT coupling involving H_g vibrational modes.[35–37] Distortions are small with the maximum value of 2 pm. We estimate the energy scale for deformation by realizing that the relaxed structure has $\Delta E_t = 170$ meV lower total energy than the starting structure with undistorted icosahedral C_{60}. Former threefold t_{1u} degeneracy of the LUMO is now removed, with t_{1u} levels split equally by $\sim$50 meV. The lowest t_{1u} orbital is doubly occupied, while the third electron goes into the central t_{1u} orbital, pinned at the Fermi level. The highest t_{1u} orbital is empty. The total energy difference, ΔE_t, has several contributions: the JT effect, the crystal-field effect, and the bond-length correction due to the LDA approximation. To estimate only the JT energy scale we compare the above ΔE_t with the one obtained for a structural relaxation with equal and fixed occupations of the t_{1u} bands, which effectively hinders the JT effect. The difference in the total energy between these two calculations is 57 meV, a typical value for the JT effect.[35,37] The proper energy scale, typical size of deformations, the right symmetry of C_{60}^{3-}, and the splitting and occupation of t_{1u} orbitals are strong indications that the observed distortion is indeed a result of the JT effect.

The residual crystal field of C_{60}^{3-} ions is immediately seen for smaller lattice parameters, i.e., when room-temperature MAK_3C_{60} lattice parameters are, for instance, multiplied by a smaller factor of 1.25. Using the same procedure as above, the structural relaxation ended up with the same deformation of the C_{60}^{3-} molecule. The only difference is that the axis of JT deformation accidentally rotated from the crystal z to y direction. This indicates that we are dealing in both cases with the JT effect and that the change in the JT deformation axis is due to the existence of several equivalent minima of the lowest JT adiabatic potential energy surface (APES).[35] These minima become nearly degenerate for large lattice expansions. On the other hand, when lattice parameters are reduced down toward experimental MAK_3C_{60} values, the orthorhombic crystal field starts to play a role by making some of the APES minima deeper, thus promoting one specific JT deformation.

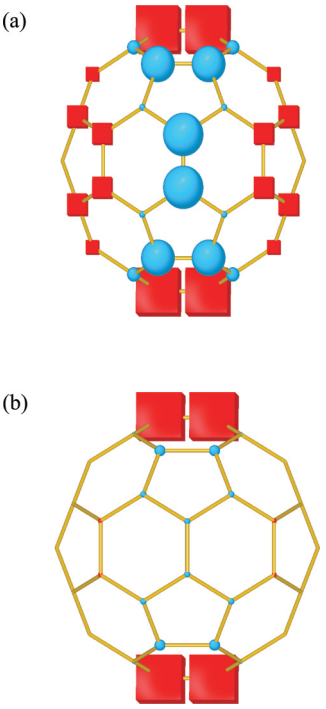

FIG. 3. (Color online) Radial molecular distortions of C_{60}^{3-} ions in (a) orthorhombic C_{60}^{3-} expanded structure, (b) K_3C_{60} orthorhombic environment. The size of blue circles and red squares is proportional to the amount of positive and negative deviations from the mean C_{60} radius at a given carbon site, respectively.

Adding potassium atoms to the above C_{60}^{3-} structure results in an artificial orthorhombic K_3C_{60} where even stronger orthorhombic crystal field due to the close contact between the K^+ and C_{60}^{3-} ions are expected. The structural optimization of the C_{60} carbon positions when starting from the JT distorted C_{60}^{3-} atomic positions [Fig. 3(a)] leads to deformations of the C_{60} molecule shown in Fig. 3(b). Molecular deformations are slightly different because the crystal field additionally lifts the t_{1u} degeneracy, hence producing a pseudo-JT effect. Nevertheless, the resulting symmetry remains D_{2h}, and the maximal distortions of 2.3 pm are similar to the previous cases. The same holds for the total energy lowering, $\Delta E_t = 140$ meV. The JT effect is obviously still dominant over orthorhombic crystal field, which represents a smaller contribution to the total energy. The important message of this part is thus that the energy scale of the JT effect is $E_{JT} \approx 60$ meV and that for the experimental unit-cell volumes a comparably weak crystal field favors a particular C_{60}^{3-} pseudo-JT deformation.

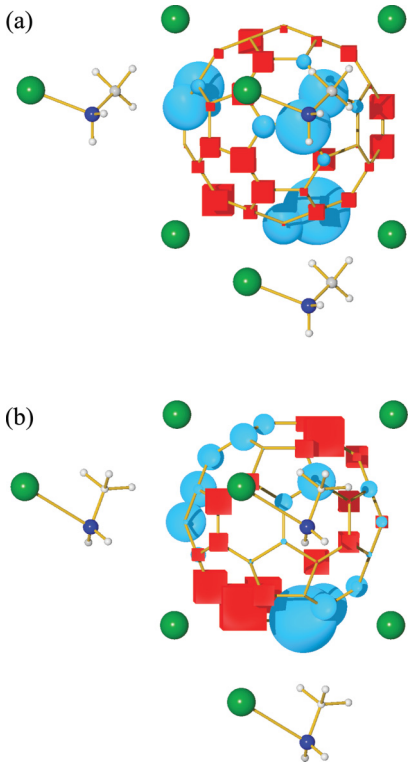

FIG. 4. (Color online) C_{60} radial deformations of MAK_3C_{60} for (a) room-temperature structure with relaxed C_{60} atom positions only and (b) completely relaxed room-temperature structure. Blue spheres correspond to inward distortions of the C_{60} cage, and red boxes represent outward cage distortions. The sizes of the markers scale linearly with the amount of distortion.

C. Methylamine-C_{60} interaction

In the MAK_3C_{60} structure, methyl protons of the MA-K^+ groups approach C_{60}^{3-} anions at very short distances, and, based on this observation, suggestions about the weak hydrogen bond were formulated in the literature.[18] Such close contacts are expected to lead to rather strong crystal fields and, according to the above discussion, to also affect strongly the pseudo-JT effect. It is not *a priori* clear which of the two effects is dominant in this structure. Therefore, C_{60}^{3-} deformations are now investigated in the room-temperature MAK_3C_{60} structure where only C_{60} carbon atoms are allowed to relax. As expected, the presence of MA molecules has a dramatic effect on the C_{60}^{3-} shape [Fig. 4(a)]. The maximal cage distortions are significantly larger than in the previous cases: They reach up to 3.4 pm, and the total energy is reduced by $\Delta E_t = 303$ meV during the structural optimization. In addition, even the D_{2h} symmetry of the distorted C_{60} molecule is lost. The maximal distortions are found for carbons facing methyl protons, at a closest-approach distance of 226 pm. Dramatically larger distortions compared to those obtained for C_{60}^{3-} or even for orthorhombic K_3C_{60} structure indicate that the additional crystal field produced by MA-K^+ groups plays a dominant role over the JT effect in MAK_3C_{60}.

We also address the possible hydrogen-bond formation by relaxing all atomic positions, including those of MA-K^+ groups. Hydrogen-bond traces can be detected on the tiny deformation of MA where C-H bond lengths of the CH_3 group are 110.3, 110.4, and 110.6 pm, the last one corresponding to the hydrogen with the closest contact to the fullerene molecule. However, with the structural relaxation, the MA-K^+ group rotates slightly away from the fullerene molecule, increasing the nearest H-C_{60} distance to 228.5 pm, i.e., by 2.7 pm longer than in the experimental structure [Fig. 4(b)]. This distance still remains in the typical hydrogen-bond length range, but the C_{60}^{3-}-methyl proton contact elongation indicates that such a bond must be very weak, if it exists at all.

D. Magnetic interactions

The above analysis points toward strong crystal fields and resulting steric C_{60}^{3-} deformations in MAK_3C_{60} arising from the MA-C_{60}^{3-} interactions. The remaining question to be addressed is how these effects influence the low-temperature magnetic properties. The appropriate starting point is to construct an effective tight-binding model for the t_{1u} bands and then relate the transfer integrals to the exchange coupling constants. To do so, we proceed by switching to the maximally localized Wannier orbitals (WOs).[24] Setting the energy window to the range around the DFT t_{1u} band (Fig. 1) we obtain three WOs, each one localized on the same C_{60} molecule. Close to the fullerene cage, a typical WO (Fig. 5) has the characteristic look of an appropriate combination of carbon $2p_z$ orbitals.[38] The orbital of Fig. 5 resembles the DFT electron density obtained at the Γ point. The distribution of $2p_z$-like orbitals complies with the expected t_{1u} symmetry. The other WOs (not shown) have a similar shape, but different orientations. Based on these WOs, we compute their on-site energies and transfer integrals between neighboring C_{60} from the Kohn-Sham Hamiltonian as[24]

$$t_{\alpha\beta}(\boldsymbol{R}_i) = \langle w(0,\alpha)|H_{\mathrm{KS}}|w(\boldsymbol{R}_i,\beta)\rangle. \quad (1)$$

Here $w(\boldsymbol{R}_i,\alpha)$ is a αth WO, and $\boldsymbol{R}_i$ is a lattice translation vector. For $\boldsymbol{R}_i = 0$ Eq. (1) gives the on-site WO energies and for $\boldsymbol{R}_i \neq 0$ Eq. (1) yields nine transfer integrals for each pair of neighboring C_{60} molecules. By diagonalizing the tight-binding model, we verify that the obtained on-site energies and transfer integrals reproduce correctly the DFT electronic band structure as shown by red solid line in Fig. 1(a).

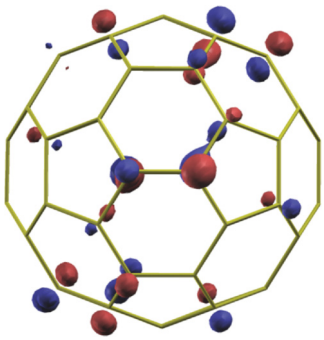

FIG. 5. (Color online) A maximally localized Wannier orbital obtained for the MAK_3C_{60} structure. A isowave function surface at levels $\pm 65\%$ of maximal value is depicted in red and blue for the positive and negative phase, respectively.[39]

TABLE I. Exchange coupling constants for the experimental room-temperature structure [Fig. 4(a)] and the relaxed structure [Fig. 4(b)]. See text for details.

Neighbors	$J_{\text{Exp.structure}}$ (meV)	J_{Relaxed} (meV)
1: (1 1 0)	0.03	0.06
2: (1 0 1)	0.02	0.02
3: (0 1 1)	**1.94**	0.01
4: (1 0 −1)	**1.89**	**3.07**
5: (0 1 −1)	0.00	0.73
6: (1 −1 0)	0.22	0.72

We note that the computed on-site tight-binding Hamiltonian has nonzero off-diagonal elements, indicating hybridization within the obtained set of WOs. By changing basis to an equivalent one where the on-site Hamiltonian becomes diagonal, we derive a new set of WOs with well-defined on-site energies. There are two indications that the new set of WOs is appropriate for our purposes: (1) the new WOs still reproduce band structure and (2) in the Mott-insulating limit such WOs are a good approximation for the localized t_{1u} electronic orbitals with well-defined on-site energies, in our case separated by 32 and 67 meV.

To estimate the exchange coupling constants we focus only on the transfer integrals of the second WO, the half-filled one at intermediate energy. The neglect of the other (interband) hopping elements between neighboring C_{60} sites amounts to neglecting interband transitions. This selection can be justified by noting that (1) the retained WO is mainly responsible for the DOS at the Fermi level [see Fig. 1(a)] and (2) in a picture where the Coulomb repulsion is the dominating interaction, the intermediate orbital hosts the unpaired spin in the spin-1/2 state of each C_{60}^{3-} molecular unit, with lower fully occupied and upper empty orbital. Within this approximation we estimate the interfullerene exchange coupling constants with Hubbard's expression $J_{ij} = 4t_{ij}^2/U$, where we take $U =$ 1 eV. For the considered MAK_3C_{60} structure the strongest exchange couplings $J_3 = J_4 = 1.9$ meV are found for nearest C_{60} neighbors along the (0 1 1) and (1 0 −1) directions. We stress that these J are of the right order of magnitude as estimated from the measured Curie-Weiss temperature $\Theta = 86$ K.[31] All other exchange constants are much weaker, not exceeding $0.12J_3$; see Table I.

The obtained exchange network indicates a quasi-two-dimensional magnetic structure of MAK_3C_{60}. Low dimensionality could account for the reduced experimental Néel temperature. However, although this is certainly a viable possibility, we stress that this conclusion is based on the high-temperature crystal structure. Since we proved that the interaction between MA and C_{60}^{3-} is the governing factor for pseudo-JT effect, we stress at this point that the low-temperature exchange network may in fact be different. How sensitive interfullerene exchange interactions are on the precise position of MA-K^+ groups becomes immediately evident when we consider relaxed DFT structure with a slightly rotated MA-K^+ groups [Fig. 4(b)]. For this structure the strongest exchange is $J_4 = 3$ meV, but now along (1 0 −1). The quasi-low-dimensional picture seems to still hold since the next two strongest interactions are much weaker, i.e., $J_5 = 0.24J_4$ along (0 1 −1), and $J_6 = 0.23J_4$ along (1 −1 0). All other exchange interactions are negligible (Table I). We stress that in all these structures the considered MA-K^+ order is ferro-orientational. Any deviation from this MA-K^+ configuration, for example, antiferro-orientational MA-K^+ order as the candidate for the low-temperature MAK_3C_{60} structure, could significantly change the quasi low-dimensional character of our system. Moreover, if a certain degree of disorder in MA-K^+ orientations is present, then one would anticipate also a distribution of exchange coupling constants, and an even smaller ordered moment. That would explain the static magnetic order with a broad-local-field distribution measured by μSR.[22] This situation is somehow reminiscent of ferromagnetic TDAE-C_{60}, where disorder in JT deformations has been argued to be responsible for the reduced order parameter[40–42] and broad distribution of local magnetic fields also measured in μSR experiment, for instance.[43] We conclude that relative orientation of neighboring cage deformations is an essential factor in interfullerene exchange coupling in MAK_3C_{60}. Judging from the experimental high-temperature structure, MAK_3C_{60} may even show low-dimensionality effects, thus explaining the reduced T_N. However, at low temperatures other relative orientations of cage deformations may change magnetic dimensionality and even suppression of T_N due to disorder effects cannot be excluded at this stage. Further progress in understanding of magnetic properties of MAK_3C_{60} would be possible only when the low-temperature crystalline structure of MAK_3C_{60} is known.

IV. CONCLUSIONS

Antiferromagnetic Mott-Hubbard insulating MAK_3C_{60} has been studied by means of DFT calculations. We found the pronounced orthorhombic crystal field anisotropy in the electronic structure and judging from $\Delta/W = 0.29$ MAK_3C_{60} should be deep in the insulating part of the phase diagram. Comparisons between different orthorhombic structures demonstrate that the JT effect is present and that its energy is around 60 meV. However, the interaction between cointercalated MA molecules and C_{60}^{3-} anions is in MAK_3C_{60} significantly stronger than pseudo-JT effect and lowers the energy of deformed structure by ∼300 meV. The presence of strong steric effects should be responsible for the suppression of T_N. Calculations based on the high-temperature structure with imposed ferro-orientational order of MA-K^+ groups suggest low dimensionality in magnetic exchange. However, other explanations such as a disorder in C_{60}^{3-} deformations cannot be excluded at this stage. A similar interplay of Mott and JT physics is believed to play an important role in the superconductivity of underdoped cuprates. In the present study we emphasize the importance of JT effect in strongly correlated C_{60}^{3-} structures and set it as one of the most important parameters for the high-temperature superconductivity in fulleride salts.

ACKNOWLEDGMENTS

We thank Gianluca Giovannetti for many stimulating discussions about these DFT results. This work was supported in part by the Slovenian Research Agency through project

No. J1-2284. E.T. and D.A. acknowledge the financial support by the European Union FP7-NMP-2011-EU-Japan project LEMSUPER under contract no. 283214. D.A. also acknowledges the support of the Institute of Advanced Study (IAS) and Chemistry Department of the Durham University through Durham International Senior Research Fellowship.

*anton.potocnik@ijs.si
†nicola.manini@mi.infm.it
‡erio.tosatti@sissa.it

[1] R. Mitsuhashi, Y. Suzuki, Y. Yamanari, H. Mitamura, T. Kambe, N. Ikeda, H. Okamoto, A. Fujiwara, M. Yamaji, N. Kawasaki, Y. Maniwa, and Y. Kubozono, Nature (London) **464**, 76 (2010).
[2] A. Y. Ganin, Y. Takabayashi, Y. Z. Khimyak, S. Margadonna, A. Tamai, M. J. Rosseinsky, and K. Prassides, Nat. Mater. **7**, 367 (2008).
[3] C. H. Pennington and V. A. Stenger, Rev. Mod. Phys. **68**, 855 (1996).
[4] O. Gunnarsson, Rev. Mod. Phys. **69**, 575 (1997).
[5] M. Fabrizio and E. Tosatti, Phys. Rev. B **55**, 13465 (1997).
[6] R. W. Lof, M. A. van Veenendaal, B. Koopmans, H. T. Jonkman, and G. A. Sawatzky, Phys Rev. Lett. **68**, 3924 (1992).
[7] Y. Iwasa and T. Takenobu, J. Phys.: Condens. Matter. **15**, R495 (2003).
[8] P. Durand, G. R. Darling, Y. Dubitsky, A. Zaopo, and M. J. Rosseinsky, Nature Mater. **2**, 605 (2003).
[9] A. Y. Ganin, Y. Takabayashi, P. Jeglič, D. Arčon, A. Potočnik, P. J. Baker, Y. Ohishi, M. T. McDonald, M. D. Tzirakis, A. McLennan, G. R. Darling, M. Takata, M. J. Rosseinsky, and K. Prassides, Nature (London) **466**, 211 (2010).
[10] Y. Takabayashi, A. Y. Ganin, P. Jeglič, D. Arčon, T. Takano, Y. Iwasa, Y. Ohishi, M. Takata, N. Takeshita, K. Prassides, and M. J. Rosseinsky, Science **323**, 1585 (2009).
[11] P. Jeglič, D. Arčon, A. Potočnik, A. Y. Ganin, Y. Takabayashi, M. J. Rosseinsky, and K. Prassides, Phys. Rev. B **80**, 195424 (2009).
[12] Y. Ihara, H. Alloul, P. Wzietek, D. Pontiroli, M. Mazzani, and M. Riccò, Phys. Rev. Lett. **104**, 256402 (2010).
[13] Y. Ihara, H. Alloul, P. Wzietek, D. Pontiroli, M. Mazzani, and M. Riccò, Eur. Phys. Lett. **94**, 37007 (2011).
[14] C. W. Chu, Nat. Phys. **5**, 787 (2009).
[15] M. Capone, M. Fabrizio, C. Castellani, and E. Tossatti, Rev. Mod. Phys. **81**, 943 (2009).
[16] M. J. Rosseinsky, D. W. Murphy, R. M. Fleming, and O. Zhou, Nature (London) **364**, 425 (1993).
[17] T. Takenobu, T. Muro, Y. Iwasa, and T. Mitani, Phys. Rev. Lett. **85**, 381 (2000).
[18] A. Y. Ganin, Y. Takabayashi, C. A. Bridges, Y. Z. Khimyak, S. Margadonna, K. Prassides, and M. J. Rosseinsky, J. Am. Chem. Soc. **128**, 14784 (2006).
[19] O. Gunnarsson, E. Koch, and R. M. Martin, Phys. Rev. B **54**, R11026 (1996).
[20] N. Manini, G. E. Santoro, A. Dal Corso, and E. Tosatti, Phys. Rev. B **66**, 115107 (2002).
[21] K. Prassides, S. Margadonna, D. Arčon, A. Lappas, H. Shimoda, and Y. Iwasa, J. Am. Chem. Soc. **121**, 11227 (1999).
[22] Y. Takabayashi, A. Y. Ganin, M. J. Rosseinsky, and K. Prassides, Chem. Commun. 820 (2006).
[23] P. Giannozzi, S. Baroni, N. Bonini, M. Calandra, R. Car, C. Cavazzoni, D. Ceresoli, G. L. Chiarotti, M. Cococcioni, I. Dabo, A. Dal Corso, S. Fabris, G. Fratesi, S. de Gironcoli, R. Gebauer, U. Gerstmann, C. Gougoussis, A. Kokalj, M. Lazzeri, L. Martin-Samos, N. Marzari, F. Mauri, R. Mazzarello, S. Paolini, A. Pasquarello, L. Paulatto, C. Sbraccia, S. Scandolo, G. Sclauzero, A. P. Seitsonen, A. Smogunov, P. Umari, and R. M. Wentzcovitch, J. Phys.: Condens. Matter **21**, 395502 (2009).
[24] A. A. Mostofi, J. R. Yates, Y. S. Lee, I. Souza, D. Vanderbilt, and N. Marzari, Comput. Phys. Commun. **178**, 685 (2008).
[25] D. Arčon, A. Y. Ganin, Y. Takabayashi, M. J. Rosseinsky, and K. Prassides, Chem. Mater. **20**, 4391 (2008).
[26] S. Margadonna, K. Prassides, H. Shimoda, T. Takenobu, and Y. Iwasa, Phys. Rev. B **64**, 132414 (2001).
[27] O. Gunnarsson, *Alkali-Doped Fullerides* (World Scientific, Singapore, 2004).
[28] R. C. Haddon, L. E. Brus, and K. Raghavachari, Chem. Phys. Lett. **125**, 459 (1986).
[29] R. Macovez, M. R. C. Hunt, A. Goldini, M. Pedio, and P. Rudolf, J. Elect. Spect. Rel. Phen. **183**, 94 (2011), and references therein.
[30] D. Arčon, M. Pregelj, A. Zorko, A. Y. Ganin, M. J. Rosseinsky, Y. Takabayashi, K. Prassides, H. van Tol, and L.-C. Brunel, Phys. Rev. B **77**, 035104 (2008).
[31] A. Y. Ganin, Y. Takabayashi, M. Pregelj, A. Zorko, D. Arčon, M. J. Rosseinsky, and K. Prassides, Chem. Mat. **19**, 3177 (2007).
[32] R. Colman, Y. Takabayashi, A. Y. Ganin, K. Prassides, M. J. Rosseinsky, A. Potočnik, A. Zorko, P. Jeglič, and D. Arčon (unpublished).
[33] F. Negri, G. Orlandi, and F. Zerbetto, Chem. Phys. Lett. **144**, 31 (1988).
[34] M. M. Khaled, R. T. Carlin, P. C. Trulove, G. R. Eaton, and S. S. Eaton, J. Am. Chem. Soc. **116**, 3465 (1994).
[35] C. C. Chancey and M. C. M. O'Brien, *The Jahn-Teller Effect in* C_{60} *and Other Icosahedral Complexes* (Princeton University Press, Princeton, 1997).
[36] A. Auerbach, N. Manini, and E. Tosatti, Phys. Rev. B **49**, 12998 (1994).
[37] N. Manini, E. Tosatti, and A. Auerbach, Phys. Rev. B **49**, 13008 (1994).
[38] Y. Nomura, K. Nakamura, and R. Arita, Phys. Rev. B **85**, 155452 (2012).
[39] A. Kokalj, Comp. Mater. Sci. **28**, 155 (2003). Code available from http://www.xcrysden.org.
[40] D. Mihailović, D. Arčon, P. Venturini, R. Blinc, A. Omerzu, and P. Cevc, Science **268**, 400 (1995).
[41] R. Blinc, P. Jeglič, T. Apih, J. Seliger, D. Arčon, and A. Omerzu, Phys. Rev. Lett. **88**, 086402 (2002).
[42] P. Jeglič, R. Blinc, T. Apih, A. Omerzu, and D. Arčon, Phys. Rev. B **68**, 184422 (2003).
[43] A. Lappas, K. Prassides, K. Vavekis, D. Arčon, R. Blinc, P. Cevc, A. Amato, R. Feyerherm, F. N. Gygax, and A. Schenck, Science **267**, 1799 (1995).